Journal of the Serbian Chemical Society

JSCS-info@shd.org.rs • www.shd.org.rs/JSCS

J. Serb. Chem. Soc. 76 (9) 1283–1294 (2011)
JSCS–4203

UDC 546.26–037:54–188:544.723.2:543.552
Original scientific paper

Influence of chemical agents on the surface area and porosity of active carbon hollow fibers

LJILJANA M. KLJAJEVIĆ[1]*, VLADISLAVA M. JOVANOVIĆ[2#], SANJA I. STEVANOVIĆ[2#], ŽARKO D. BOGDANOV[1] and BRANKA V. KALUDJEROVIĆ[1]

[1]*University of Belgrade, Vinča Institute of Nuclear Sciences, P. O. Box 522, 11001 Belgrade and* [2]*ICTM – Institute of Electrochemistry, University of Belgrade, P. O. Box 473, 11000 Belgrade, Serbia*

(Received 26 February 2010, revised 31 May 2011)

Abstract: Active carbon hollow fibers were prepared from regenerated polysulfone hollow fibers by chemical activation using: disodium hydrogen phosphate 2-hydrate, disodium tetraborate 10-hydrate, hydrogen peroxide, and diammonium hydrogen phosphate. After chemical activation fibers were carbonized in an inert atmosphere. The specific surface area and porosity of obtained carbons were studied by nitrogen adsorption–desorption isotherms at 77 K, while the structures were examined with scanning electron microscopy and X-ray diffraction. The activation process increases these adsorption properties of fibers being more pronounced for active carbon fibers obtained with disodium tetraborate 10-hydrate and hydrogen peroxide as activator. The obtained active hollow carbons are microporous with different pore size distribution. Chemical activation with phosphates produces active carbon material with small surface area but with both mesopores and micropores. X-ray diffraction shows that besides turbostratic structure typical for carbon materials, there are some peaks which indicate some intermediate reaction products when sodium salts were used as activating agent. Based on data from the electrochemical measurements the activity and porosity of the active fibers depend strongly on the oxidizing agent applied.

Keywords: carbon hollow fibers; chemical activation; adsorption; cyclic voltammetry.

INTRODUCTION

Various kinds of porous carbon materials with a wide range of structures, compositions and properties are widely produced and they can be used as adsorbents, catalytic supports, *etc*.[1] In order to obtain a high surface area, physical or/and chemical activation processes of material have usually been employed. Chemical activation offers some advantages over physical activation, such as: the

* Corresponding author. E-mail: ljiljana@vinca.rs
# Serbian Chemical Society member.
doi: 10.2298/JSC100226112K

use of lower temperatures and heat treatment times, usually it consists of one stage and the obtained carbon yields are generally higher. The disadvantages are the need for a washing step of the activated material to remove the chemical agent and the inorganic reaction products, as well as the more corrosive nature of the chemical agents used in comparison to CO_2 or steam.

Through the activation process, depending on the nature of the organic precursor and process parameters, various active carbons have been prepared and various applications developed. In addition to classical granular or powder active carbon forms, there are new forms of active carbons: fibers and textiles, carbon molecular sieves, porous carbon membranes, carbon aerogels or cryogels, and carbon hollow fibers (CHF).[1–3]

Carbon membranes with useful characteristics and numerous advantages have great potential to be widely used in gas separation processes, especially carbon hollow fiber membranes [4]. There are numerous applications of hollow fiber technology for the separation and purification in both industry and medicine, including the preparation of drinkable, high quality water, for the pharmaceutical industry (hemodialyzers), gas separation for industrial application, *etc*.

Hollow fibers can be used to prepare microcapillary catalytic reactor elements. These reactors could be prepared in the form of composites with glassy carbon as the matrix[5] or with a porous carbon matrix.[6] Considering flows, mass and energy balances for an exothermic reaction inside a single fiber, better heat transport, shorter diffusion lengths and small axial dispersion were obtained when compared to classic catalytic tube reactors.[5]

Hollow-fiber carbon membranes were prepared and used as the support media for a platinum catalyst.[7]

Amongst the precursors applied for the preparation of carbon hollow fibers are polysulfone (PSF),[8,9,10] cellulose,[10,11] mesophase pitch,[12] polyacrylonitrile (PAN),[3,13] polyetherimides[14] and polyimides.[15]

Active carbon hollow fibers compared to classic active carbon possess higher geometric area to volume ratios, which improves the heat and a mass transport.

Studies of active carbon hollow fibers (ACHF) formation are, however, quite scarce. Some research was realized with PAN as the precursor,[3] and others by filling or impregnating hollow fibers with active carbon.[8,9] ACHF were obtained when PAN hollow fibers were pretreated with diammonium hydrogen phosphate and then further oxidized in air, carbonized in nitrogen, and activated with carbon dioxide.[3]

Generally, in the literature, there are several activating agents used for the chemical activation of carbon precursor material, such as phosphoric acid,[16] zinc chloride,[17] alkaline carbonates[18,19] and more recently alkaline hydroxides.[20]

This present work investigates the effect of different chemical agents on the formation of microporous and mesoporous structures of the obtained active

carbon hollow fibers through measurement of their microstructure, adsorption and electrochemical characteristics.

EXPERIMENTAL

The polysulfone hollow fibers used as the raw material in this study were taken from a hollow fiber dialyzer supplied by Hemofarm AD, Vršac in cooperation with Fresenius, Bad Homburg, Germany. The hollow fibers were roughly cut to about 1 cm long fibers. The approximately same mass of cut fibers were soaked in 15 % aqueous solutions of $Na_2HPO_4 \cdot 2H_2O$ (1), $Na_2B_4O_7 \cdot 10H_2O$ (2), H_2O_2 (3), or $(NH_4)_2HPO_4$ (4) for one hour.

The ratio of the mass of the chemical agents in solution to the mass of the used hollow fibers was about 5. The mixtures were then filtered and the remaining wet fibers were dried at 353 K for about 6 h. The impregnation yield was calculated as the ratio of the mass difference of the hollow fibers after and before drying and the mass of the hollow fibers before drying.

These fibers were carbonized in a horizontal tubular furnace under an Ar flow up to 1173 K at a heating rate of 5 K min^{-1} and maintained at the final temperature for 1 h. After cooling under an Ar flow, the ACHF samples were washed with distilled water. The final wash was at elevated temperature (333 K) for 1 h. After filtration, the wet fibers were dried in an oven at 353 K for about 6 h.

The samples are designated ACHF1 ACHF2, ACHF3 and ACHF4, according to the ordinal number of the used chemical agent (number in parentheses, next to chemical agent).

The adsorption characteristics of ACHF were experimentally and numerically characterized according to their surface area, pore volume and pore sizes. The crystalline structure was examined by X-ray diffraction analysis (XRD) and morphology investigated by scanning electron microscopy (SEM).

The adsorption characteristics were determined from N_2 adsorption/desorption isotherms at 77 K using the gravimetric McBain balance method. Before obtaining adsorption isotherms, the ACHF samples were degassed at a temperature of 523 K to remove any contaminants that may be present on their surface. The values of specific surface area (S_{BET}) were calculated from the adsorption data applying the standard Brunauer–Emmet–Teller (BET) Equation.[21] The BET surface areas were assessed by applying relative pressures ranging from 0.01 to 0.15. The total pore volume V_{tot} was estimated by the Gurwitsch Rule[21] using the quantity adsorbed close to saturation, *i.e.*, the liquid volumes of N_2 at a relative pressure $p/p_0 = 0.95$.

The micropores volume (V_{DR}) and characteristic adsorption energy (E_0) were calculated by application of the Dubinin–Radushkevich (D–R) Equation.[22]

Using the Stoeckli Formulas based on the D–R Equation, the average width of the slit-shaped pores (L_0) was calculated. This pore width was used to calculate the surface area of the micropores (S_L).[23]

The average micropore width (W_m) was also calculated from the McEnaney Equation using the parameter of the D–R isotherm (E_0),[24] followed by the calculation of the surface area of the micropores (S_W).

The high resolution α_s-plot and the method proposed by Kaneko *et al.*[25] were used to calculate the micropore volume ($V_{\alpha s}$) and the external surface area (S_{ext}) as well as the total surface area (S_{tot}). Non-graphitized carbon black BP 280 (S_{BET} = 40.2 m^2 g^{-1}) was used as the reference adsorbent. The micropore surface (S_{mic}) for the mesoporous materials were calculated by subtracting S_{ext} from S_{tot}.

The effective pore size distribution (L) was calculated according to the Horvath and Kawazoe (HK) method. This function gives the effective pore size for micropores, the values

of which are between 0.35 and 1.4 nm.[26] The Orr and Dalla Valle's modification of the Pierce method was used for the calculation of the mesopore size distribution (w).[21] Both methods were applied to the appropriate part of the desorption branch of the N_2 isotherm.

The XRD analysis was performed with a Siemens D500 diffractometer using Ni-filtered CuKα radiation. The interlayer distance (d_{002}) and crystallite height (L_c) were determined from the 002 diffraction peak, and the crystallite width, size (L_a), along the basal plane, from the θ position of the (100) diffraction peak. The calculations were performed with the Bragg and the Scherer Formulas.[1]

The texture of the obtained ACHF was analyzed by scanning electron microscopy (SEM) using a JEOL JSM-35 instrument.

The investigated carbon fibers were also characterized by cyclic voltammetry. The fibers were ground and applied in the form of a thin layer from aqueous suspensions onto a polished glassy carbon disk substrate. The suspensions were prepared by ultrasonic homogenization for 1 h. The loading in all experiments was ≈170 μg cm^{-2}. In order to provide firm attachment, the fibers layer was covered by Nafion® from a 100:1 (v/v) mixture of water and Nafion®ethanol solution (5 mass %, 1100 E.W., Aldrich). After each application, the electrode was dried in an oven at 65 °C. Cyclic voltammetry (CV) measurements were performed in 0.5 mol dm^{-3} H_2SO_4 with sweep rates of 100, 50, 25 and 5 mV s^{-1}. All experiments were realized at room temperature with a Pt wire as the counter electrode and saturated calomel electrode (SCE) as the reference. All the potentials are given *versus* SCE. The electrolyte was purged with purified nitrogen prior to each experiment.

RESULTS AND DISCUSSION

Nitrogen adsorption/desorption isotherms, depending on the activated agent, are shown in Fig. 1. These isotherms show that the used chemical agents were more or less effective for activation process, allowing active carbons with very different adsorbed amounts (n) and isotherm shapes to be obtained, which are indicative of different specific surface areas, micropore volumes and total pore volumes (Table I), as well as pores sizes (Table II).

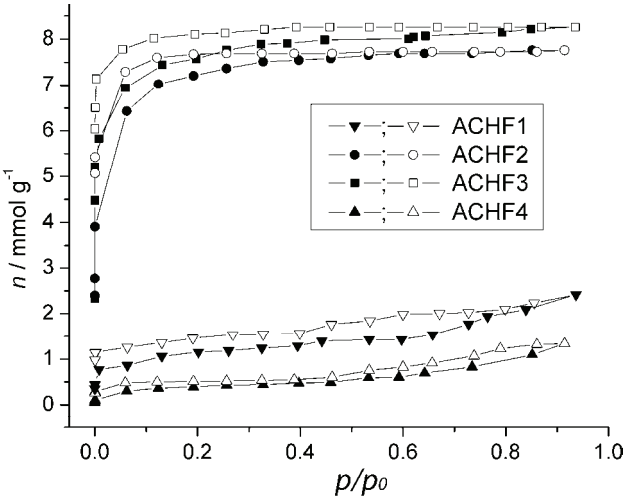

Fig. 1. Nitrogen isotherms for carbon hollow fibers activated with different agents: solid symbols – adsorption, open symbols – desorption.

TABLE I. Adsorption characteristics of carbon hollow fibers activated with different agents

Sample	S_{BET} $m^2 g^{-1}$	V_{tot} $cm^3 g^{-1}$	V_{DR} $cm^3 g^{-1}$	S_{mic} $m^2 g^{-1}$	V_{os} $cm^3 g^{-1}$	S_{ext} $m^2 g^{-1}$	S_{tot} $m^2 g^{-1}$
ACHF1	88	0.084	0.033	43	0.041	41	84
ACHF2	600	0.269	0.238	558	0.262	6	564
ACHF3	632	0.286	0.245	613	0.271	12	625
ACHF4	32	0.046	0.014	16	0.005	11	27

TABLE II. Values for micropore sizes and surface area of the micropores calculated using the DR characteristic adsorption energy

Sample	E_0 / kJ mol^{-1}	L_0 / nm	S_L / $m^2 g^{-1}$	W_m / $cm^3 g^{-1}$	S_W / $m^2 g^{-1}$
ACHF1	19.44	1.40	47	1.28	51
ACHF2	22.35	1.08	439	1.06	449
ACHF3	25.11	0.89	550	0.88	555
ACHF4	16.61	1.98	14	1.55	18

Two types of isotherms were clearly observed. Carbons ACHF1 and ACHF4 activated by phosphate salts ($Na_2HPO_4 \cdot 2H_2O$ and $(NH_4)_2HPO_4$, respectively) exhibit type IV isotherms, according to the IUPAC classification and indicate the occurrence of capillary condensation in the pores. The limiting uptake over the range of high relative pressures p/p_0 resulted in a plateau on the isotherm (Fig. 1), which indicates complete pore filling. The hysteresis loops in both cases are Type H4, according to the IUPAC classification and indicate the presence of mesopores and slit-shaped pores, but the pore size distribution is mainly in the range of micropores.[21] This was confirmed by further analysis and will be discussed later.

The carbons ACHF2 and ACHF3 activated by $Na_2B_4O_7 \cdot 10H_2O$ and H_2O_2, respectively, exhibited type I isotherms, according to the IUPAC classification, which indicate microporous materials.[1,21] These isotherms exhibit low-pressure hysteresis, attributed to the irreversible uptake of adsorptive molecules in pores of about the same width as that of the adsorbate molecules, and/or swelling of non-rigid pore walls.[21] Micropore filling and high uptakes were observed at relatively low pressures (Fig. 1), because of the narrow pore width which induced high adsorption potential. The knee of the nitrogen adsorption isotherm at 77 K for the ACHF3 sample is sharper than that for the ACHF2 sample, which means that the net heat of adsorption is higher and the micropores are narrower for ACHF3 (Table II and Fig. 2).

Chemical activation increased the specific surface area significantly from $S_{BET} = 3.2\ m^2\ g^{-1}$ obtained for the carbon hollow fibers (CHF) to $S_{BET} = 632\ m^2\ g^{-1}$ obtained for the activated carbon hollow fibers ACHF3, (Table I). The presence of microporosity increases the specific surface area of an active material. Thus, the specific surface area of the microporous materials ACHF2 and ACHF3

was greatly enhanced when compared with those of the mesoporous materials ACHF1 and ACHF4 (Table I).

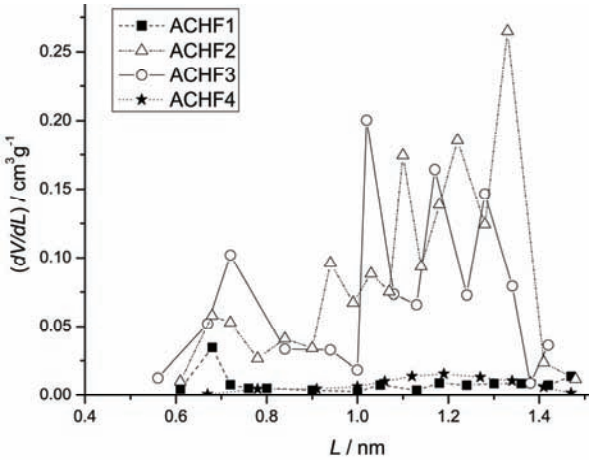

Fig. 2. Effective pore size distribution of the activated CHF calculated by the HK method.

The usage of disodium tetraborate 10-hydrate (ACHF2) and hydrogen peroxide (ACHF3) as the activating agent induced significant increases of the specific surface area and especially of the total and micropore volume. Remarkably higher micropore volume for these samples in comparison with ACHF1 and ACHF4 (Table I), was confirmed by both calculation methods α_s ($V_{\alpha s}$) and D–R ($V_{D–R}$). The values of V_{mic} obtained from these two methods are in disagreement, which was more pronounced for the mesoporous samples, especially for ACHF4. This was to be expected because the D–R method is proposed for microporous materials. The mesoporous structure of these two materials is presented by the pore size distribution in Fig. 3. However, V_{mic} for the microporous ma-

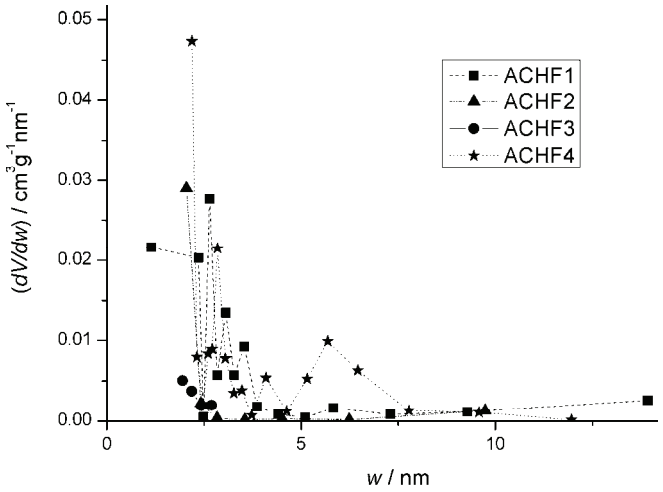

Fig. 3. Pore size distribution of activated CHF calculated using the Orr and Dalla Valle modification of the Pierce method.

terials ACHF2 and ACHF3 calculated using the D–R method was lower by about 9 % than when they are calculated using the α_s method. The reason for this could lie in the broad micropore size distribution (Fig. 2). Additionally, the fact that the α_s method is based on the standard isotherm affects that the $V_{\alpha s}$ values are expected to be more accurate than the $V_{D–R}$ values for the micropore volume.

Average width of the slit-shaped pores calculated using the parameters of D–R Equation L_0 and W_m have different values depending on the employed calculation method (Table II). The values for the micropore width obtained using the McEnaney Equation (W_m) were lower than L_0 (Stoeckli Formulas), especially for the mesoporous materials ACHF1 and ACHF4 as well as the corresponding surface area of the micropores. Of these two mesoporous materials, ACHF1 had a higher micropore surface area according to the smaller micropore size of this material (Fig. 2). The wider the micropore size is, the smaller is the micropore surface area. The activation with phosphoric salts, besides developing mesoporosity, induced wider micropore size and accordingly a low surface area of the micropores. Although the D–R Equation is more appropriate for microporous materials, the values of S_L for the mesoporous materials were in a good agreement with the values obtained by the α_s method (Tables I and II). However, the values of S_L and S_W for the microporous materials ACHF2 and ACHF3 were lower than the values obtained by the α_s method. The values S_L and S_W were calculated using the mean pore width but these materials had a broad micropore size distribution (Fig. 2).

External surface area, which presents the mesopores and the macropores surface area, was greater in the materials ACHF1 and ACHF4 than in the microporous materials ACHF2 and ACHF3, Table I. Even the presence of macropores on the surface of ACHF1 could be seen in the SEM analysis, see Fig. 4. Moreover,

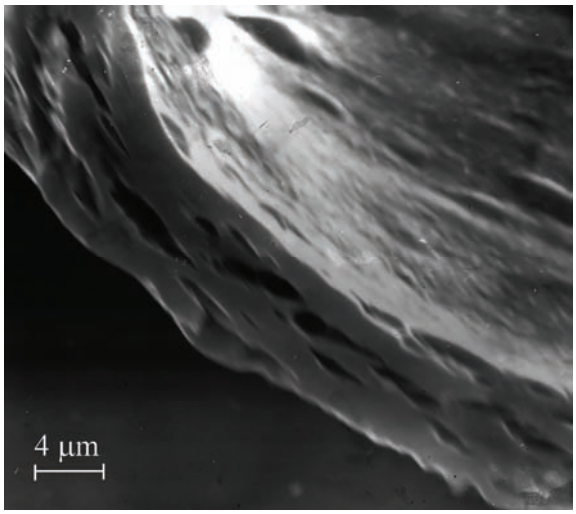

Fig. 4. SEM Micrograph for carbon hollow fibers activated by $Na_2HPO_4 \cdot 2H_2O$ – ACHF1.

the S_{ext} was almost half (ACHF1) or less than a half (ACHF4) of total surface area S_{tot}. Thus, the sodium salt as the activating agent developed a larger surface area and smaller average mesopore size (w) in the material (ACHF1) than the ammonium salt (ACHF4) of phosphoric acid (Fig. 3). The external surface area for the microporous materials ACHF2 and ACHF3 was negligible, which was confirmed by the results obtained for the pore size distribution for the mesopores (Fig. 3).

The X-ray diffraction patterns of the carbon hollow fibers (CHF) and the activated samples had features that are common to other active carbons: the two broad peaks near 2θ 24 and 42° (Fig. 5) are assigned to the (002) and (100) reflections, respectively.[1] There were some peaks for the samples ACHF1 and ACHF2 in Fig. 5 which were hard to identify and they could belong to intermediate reaction products. These peaks were only present when the sodium salts were used for the activation process.

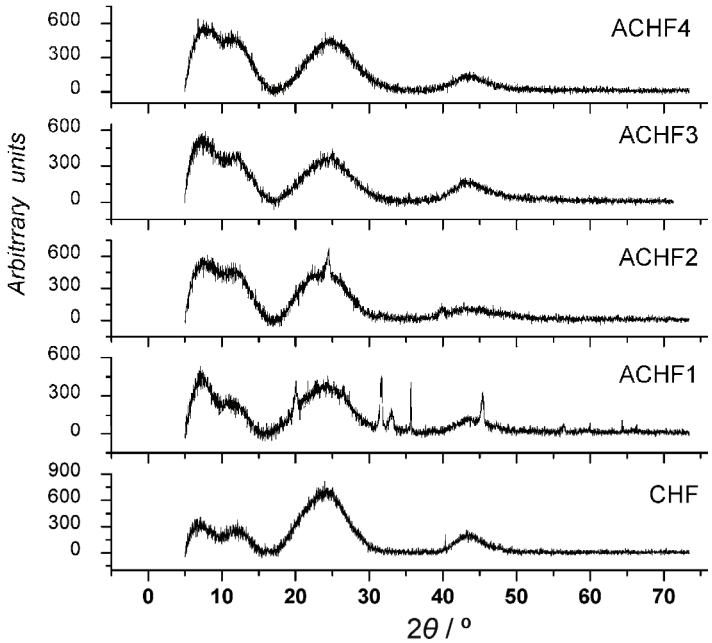

Fig. 5. X-Ray diffraction patterns of the carbon hollow fibers (CHF) and those activated with different agents.

The results of X-ray diffraction analysis of CHF before and after oxidation process are given in Table III. The d_{002} value was between 0.36 nm for ACHF4 and 0.38 nm for the ACHF2 sample, which is greater than that of graphite (0.335 nm). The crystallite height L_c was in the range of 1.05 nm for ACHF1 and 1.35 nm for the CHF sample. The values for the crystallite width L_a was between 3.43

nm for the ACHF3 and 4.57 nm for the CHF samples. Therefore, these materials had a turbostratic structure similar to that of active carbon, as well as the majority of carbonaceous materials. However, the chemical agents introduced defects in the structure of the carbon material which led to the formation of the porosity. The changes in the structure of the carbon hollow fibers that occurred on activation mainly decreased the interlayer spacing and crystallites size.

TABLE III. Results of the X-ray diffraction analysis of carbon hollow fibers (CHF) and carbon hollow fibers activated with different agents

Sample	CHF	ACHF1	ACHF2	ACHF3	ACHF4
d_{002} / nm	0.372	0.365	0.376	0.364	0.359
L_c / nm	1.35	1.25	1.11	1.10	1.07
L_a / nm	4.57	3.27	2.03	3.29	3.31
L_c/d_{002}	3.6	3.4	2.9	3	3.0

The influence of oxidizing agent used for activation of the raw hollow fibers was also analyzed by cyclic voltammetry. The steady state CVs recorded in 0.5 M H_2SO_4 of all the studied fibers are shown in Fig. 6. None of the ACHF fibers exhibited pure double layer properties. The voltammograms for ACHF1 and

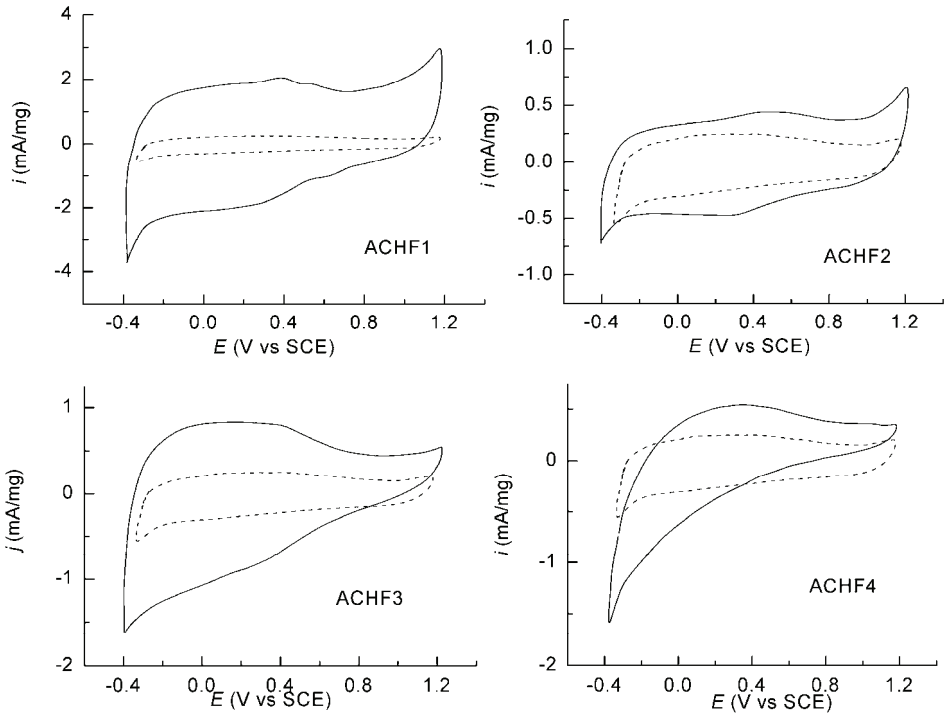

Fig. 6. Cyclic voltammograms for the carbon hollow fibers (CHF) – dashed line, and activated with different agents – solid line.

ACHF2 had a more or less defined redox peak at around 0.4 V *vs*. SCE, designating a redox reaction of carbon functional groups (mostly quinone/hydroquinone) that is characteristic for carbon materials in acidic solution.[27–30] However, the voltammograms for ACHF3 and ACHF4, although recorded in acid, were more similar to the CVs for carbon materials in alkaline solution.[31] The charge calculated from the CVs for the activated fibers ACHF1–4 was from 2 to 8 times larger in comparison to that for the raw fibers CHF. In addition, the increase in charge at the slower sweep rate, as an indication of porosity, was higher for the activated fibers. Moreover, both the increase of charge, which could be considered as a measure of activity, and the increase of the porosity of the active fibers depended on the applied oxidizing agent. Based on data from the electrochemical measurements, the activity and porosity of the active fibers was in the order ACHF1 > ACHF3 > ACHF2 ≥ ACHF4. According to the results obtained from the N_2 adsorption analysis, it seems that the external surface area S_{ext} (Table I) had a great influence on the electrochemical characteristics.

CONCLUSIONS

In conclusion, it can be stated that the chemical activation of polysulfone hollow fibers increased their specific surface area after the carbonization process. This is in dependence on which chemical agent was used. Phosphates such as disodium hydrogen phosphate 2-hydrate more and diammonium hydrogen phosphate less, have a significant influence on the formation of a mesoporous structure of the active hollow carbon fibers. It is presumed this could influence the electrochemical characteristics of these materials. Microporous active carbon hollow fibers can be obtained using hydrogen peroxide or disodium tetraborate 10-hydrate.

In the future work, it would be interesting to investigate the effects of other activation methods on the adsorption characteristics of these materials, as well as their possible application for the adsorption of various contaminants from fluids, and as catalytic supports.

Acknowledgements. This paper was financially supported by the Ministry of Education and Science of the Republic of Serbia, Contracts No. 45005 and 45012.

ИЗВОД

УТИЦАЈ ХЕМИЈСКИХ АГЕНАСА НА СПЕЦИФИЧНУ ПОВРШИНУ И ПОРОЗНОСТ АКТИВНИХ УГЉЕНИЧНИХ ШУПЉИХ ВЛАКАНА

ЉИЉАНА М. КЉАЈЕВИЋ[1], ВЛАДИСЛАВА М. ЈОВАНОВИЋ[2], САЊА И. СТЕВАНОВИЋ[2], ЖАРКО Д. БОГДАНОВ[1] и БРАНКА В. КАЛУЂЕРОВИЋ[1]

[1]Институт за нуклеарне науке "Винча", п. пр. 522 ,11001 Београд и [2]ИХТМ – Институт за електрохемију, п. пр. 473, 11000 Београд

Активна угљенична шупља влакна су добијена хемијском активацијом полисулфонских шупљих влакана помоћу раствора динатријум-водоник-фосфата-2-хидрата, динатријум-тет-

рабората 10-хидрата, водоник-пероксида и диамонијум-водоник-фосфата. Након хемијске активације, влакна су карбонизована у инертној атмосфери. Специфична површина и порозност добијених влакана су испитивана преко изотерми адсорпије–десорпције азота на 77 K, док је структура испитивана скенирајућом електронском микроскопијом и рендгенском дифракцијом. Процес активације побољшава адсорпциона својства влакана, што је нарочито изражено код активних шупљих влакана активираних помоћу динатријум-тетрабората--10-хидрата и водоник-пероксида. Активна угљенична шупља влакна су микропорозна са различитом расподелом величине пора. Хемијском активацијом фосфатима добија се активан карбонски материјал мале специфичне површине, али са мезопорозном и микропорозном структуром. Рендгено-структурна анализа, поред турбостратичне структуре, типичне за угљеничне материјале, указује на присуство неких интермедијарних једињења насталих у току процеса активације солима натријума. На основу електрохемијских мерења може се закључити да активност и порозност активних влакана строго зависе од примењеног активационог агенса.

(Примљено 26. фебруара 2010, ревидирано 31. маја 2011)

REFERENCES

1. T. J. Bandosz, M. J. Biggs, K. E. Gubbins, Y. Hattori, T. Iiyama, K. Kaneko, J. Pikunic, K. T. Thomson, in *Chemistry and Physics of Carbon*, Vol. 28, L. R. Radovic, Ed., Marcel Dekker, New York, 2003, p. 41
2. M. Inagaki, L. R. Radovic, *Carbon* **40** (2002) 2279
3. J. Sun, G. Wu, Q. Wang, *J. Appl. Poly. Sci.* **93** (2004) 602
4. A. F. Ismail, L. I. B. David, *J. Membr. Sci.* **193** (2001) 1
5. M. Mitrović, Z. Laušević, M. Petkovska, B. Kaludjerović, M. Laušević, in *The role of theory in the development of industrial catalysis*, P. Putanov, Ed., Academy of Sciences and Arts of Vojvodina, Novi Sad, Serbia, 1992, p. 21
6. B. V. Kaludjerović, V. M. Jovanović, B. M. Babić, S. Terzić, Ž. Bogdanov, *J. Optoelectron. Adv. Mater.* **10** (2008) 2708
7. R. D. Sanderson, E. R. Sadiku, *J. Appl. Polym. Sci.* **87** (2003) 1051
8. L. Y. Jiang, T.-S. Chung, R. Rajagopalan, *Carbon* **45** (2007) 166
9. Y. Li, K.-C. Loh, *J. Membr. Sci.* **276** (2006) 81
10. B. V. Kaluđerović, Lj. Kljajević, D. Sekulić, J. Stašić, Ž. Bogdanov, *Chem Ind. Chem. Eng. Q.* **15** (2009) 29
11. C. Y. Wang, M. W. Li, Y. L. Wu, C. T. Guo, *Carbon* **36** (1998) 1749
12. G. Zhu, T.-S. Chung, K.-C. Loh, *J. Appl. Polym. Sci.* **76** (2000) 695
13. S. M. Saufi, A. F. Ismail, *Membr. Sci. Tech.* **24** (Suppl.) (2002) 843
14. E. Barbosa-Coutinho, V. M. M. Salim, C. Piacsek Borges, *Carbon* **41** (2003) 1707
15. N. Tanihara, H. Shimazaki, Y. Hirayama, S. Nakanishi, T. Yoshinaga, Y. Kusuki, *J. Membr. Sci.* **160** (1999) 179
16. F. Suarez-Garcia, A. Martinez-Alonso, J. M. D. Tascon, *Microporous Mesoporous Mater.* **75** (2004) 73
17. F. Rodriguez-Reinoso, M. Molina-Sabio, *Carbon* **30** (1992) 1111
18. A. P. Carvalho, M. Gomes, A. S. Mestre, J. Pires, M. B. de Carvalho, *Carbon* **42** (2004) 672
19. J. Hayashi, M. Uchibayashi, T. Horikawa, K. Muroyama, V. G. Gomes, *Carbon* **40** (2002) 274

20. A. Linares-Solano, D. Lozano-Castello, M.A. Lillo-Rodenas, D. Cazorla-Amoros, in *Chemistry and Physics of Carbon*, Vol. 30, L. R. Radovic, Ed., Marcel Dekker, New York, 2008, p. 1
21. F. Rouquerol, J. Rouquerol, K. Sing, *Adsorption by Powders and Porous Solids*, Academic Press, London, 1999, p. 197
22. M. M. Dubinin, in *Chemistry and Physics of Carbon* Vol. 2, P. L. Walker Jr., Ed., Marcel Dekker, New York, 1996, p. 51
23. F. Stoeckli, M. V. López-Ramón, D. Hugi-Cleary, A. Guillot, *Carbon* **39** (2001) 1115
24. B. McEnaney, *Carbon* **26** (1988) 267
25. K. Kaneko, C. Ishii, H. Kanoh, Y. Hanzawa, N. Setoyama, T. Suzuki, *Adv. Colloid Interface Sci.* **76**–**77** (1998) 295
26. G. Horwat, K. Kawazoe, *J. Chem. Eng. Jpn.* **16** (1983) 470
27. K. Kinoshita, J. A. S. Bett, *Carbon* **12** (1974) 525
28. A. Dekanski, J. Stevanović, R. Stevanović, B. Ž. Nikolić, V. M. Jovanović, *Carbon* **39** (2001) 1195
29. A. B. Dekanski, V. V. Panić, V. M. Jovanović, R. M. Stevanović, *J. Power Sources* **181** (2008) 186
30. M. D. Obradović, G. D. Vuković, S. I. Stevanović, V. V. Panić, P. S. Uskoković, A. Kowal, S. Lj. Gojković, *J. Electroanal. Chem.* **634** (2009) 22
31. V. Jovanović, R. Atanasoski, B. Nikolić, *J. Serb. Chem. Soc.* **51** (1986) 611.